Key Points:
- Extreme snow water equivalent (SWE), snowmelt, and runoff potential maps were developed using a regional climate model ensemble for historical and future periods
- The magnitudes of projected extreme SWE and snowmelt decrease over the CONUS and southern Canada but increase in Alaska and northern Canada
- There is a projected decrease in snowmelt but an increase in runoff potential (e.g., rain-on-snow) in California and the Pacific Northwest

Author Contributions:
Conceptualization: Eunsang Cho, Rachel R. McCrary, Jennifer M. Jacobs
Data curation: Rachel R. McCrary
Funding acquisition: Jennifer M. Jacobs
Methodology: Eunsang Cho, Rachel R. McCrary, Jennifer M. Jacobs
Project Administration: Jennifer M. Jacobs
Resources: Rachel R. McCrary
Software: Rachel R. McCrary
Supervision: Jennifer M. Jacobs
Validation: Eunsang Cho
Visualization: Eunsang Cho
Writing – original draft: Eunsang Cho

Future Changes in Snowpack, Snowmelt, and Runoff Potential Extremes Over North America

Eunsang Cho[1,2] , Rachel R. McCrary[3], and Jennifer M. Jacobs[4,5]

[1]Hydrological Sciences Laboratory, NASA Goddard Space Flight Center, Greenbelt, MD, USA, [2]Earth System Science Interdisciplinary Center, University of Maryland, College Park, MD, USA, [3]National Center for Atmospheric Research, Boulder, CO, USA, [4]Department of Civil and Environmental Engineering, University of New Hampshire, Durham, NH, USA, [5]Earth Systems Research Center, University of New Hampshire, Institute for the Study of Earth, Oceans, and Space, Durham, NH, USA

Abstract Snowpack and snowmelt-driven extreme events (e.g., floods) have large societal consequences including infrastructure failures. However, it is not well understood how projected changes in the snow-related extremes differ across North America. Using dynamical downscaled regional climate model (RCM) simulations, we found that the magnitudes of extreme snow water equivalent, snowmelt, and runoff potential (RP; snowmelt plus precipitation) decrease by 72%, 73%, and 45%, respectively, over the continental United States and southern Canada but increase by up to 8%, 53%, and 41% in Alaska and northern Canada by the late 21st century. In California and the Pacific Northwest, there is a notable increase in extreme RP by 21% contrary to a decrease in snowmelt by 31% by the late century. These regions could be vulnerable to larger rain-on-snow floods in a warmer climate. Regions with a large variability among RCM ensembles are identified, which require further investigation to reduce the regional uncertainties.

Plain Language Summary Even though snow-driven extreme events (e.g., snowmelt floods) have large societal impacts including infrastructure failures, how much future changes in the magnitude of snow-driven extremes differ across North America is not well understood. Here, we found that the magnitudes of future extreme snow water equivalent (SWE) and snowmelt decrease over the continental United States and southern Canada but increase in Alaska and northern Canada by the late 21st century. In California and the Pacific Northwest, there is a notable increase in runoff potential (snowmelt plus precipitation) contrary to a decrease in snowmelt itself, suggesting that these regions may be vulnerable to larger rain-on-snow events in a warmer climate. Also, regions with a large variability among this study's regional climate models are identified. The large variabilities in extreme SWE and snowmelt in the western mountain regions and northern Canada as well as runoff potential in the southeastern United States require further investigation to reduce the regional uncertainties.

1. Introduction

Snowpack, the accumulated snow on the ground, is one of the fastest-changing hydrologic components under a warming climate (Barnett et al., 2005; Musselman et al., 2017). The melted water from the snowpack provides the dominant source of water for generating river flow and recharging groundwater in snow-dominant regions (Li et al., 2017). At the same time, snowmelt-driven extreme events have potentially large societal and economic impacts on local and regional communities. Extreme snowmelt including rain-on-snow (ROS) events is an important driver of severe flood events (Berghuijs et al., 2016; Villarini, 2016; Yan et al., 2018, 2019). During the last few decades, snow-related floods have impacted local communities across the United States and Canada (Stadnyk et al., 2016). The Red River of the North Basin's 1997 flood caused more than $5 billion of damages in North Dakota, Minnesota, and Canadian communities (Todhunter, 2001). The Oroville dam spillway incident in California in February 2017 was exacerbated by early snowmelt with large ROS events (Henn et al., 2020; Vano et al., 2019). In the northeastern United States and eastern Canada, snowmelt-driven floods have frequently occurred with ice-jamming, resulting in physical and economic damages to riverine communities (Rokaya et al., 2018; Yarnal et al., 1997).

Writing – review & editing: Eunsang Cho, Rachel R. McCrary, Jennifer M. Jacobs

Civil and water resources engineers rely on historical data sets when making estimates of design floods to determine the size of infrastructure (e.g., dams and bridges). The current U.S. government standard design maps such as the National Oceanic and Atmospheric Administration's National Weather Service Precipitation-Frequency Atlas 14 (NOAA Atlas 14) are based solely on liquid precipitation data with very limited guidance on snowmelt events (Fassnacht & Records, 2015; Harpold & Kohler, 2017; Yan et al., 2019). Recently, Cho and Jacobs (2020) developed 25 and 100-year return level (also known as a recurrence interval that is an estimated average time between the events to occur) snow water equivalent (SWE) and snowmelt maps using reliable long-term gridded SWE products and compared these to the NOAA Atlas 14 standard design maps over the continental United States. They found that their snowmelt design values exceeded the standard rainfall design values in 23% of the area in the 44 United States where the standard maps are available. They emphasized that in most snow-dominant regions, extreme runoff potential (RP; snowmelt plus precipitation; e.g., ROS), is larger than the snowmelt itself, indicating that rainfall (or mixed-phase precipitation) during snowmelt is a major contributor to larger snow-driven extreme events. Considering a warmer climate in the future, more precipitation will likely occur as rainfall instead of snowfall, subsequently resulting in more intense, large ROS events relative to current conditions (Musselman et al., 2018). Thus, guidance is needed to design North American infrastructure to accommodate future snow-driven extreme events (Diffenbaugh, 2017; Diffenbaugh et al., 2013).

Projected extreme precipitation is expected to increase by around 20% by the end of the 21st century across the United States under a higher greenhouse gas emission scenario (the Representative Concentration Pathway [RCP] 8.5) (Easterling et al., 2017). In the winter and spring seasons, the north-central and northeastern United States and Alaska are projected to receive more seasonal precipitation by up to 30% relative to the 1976–2005 average (Easterling et al., 2017). In Canada, winter precipitation (December to February) is also projected to increase by around 24% over the 21st century, with larger percentage changes in northern Canada (30%; Bush & Lemmen, 2019). As temperature is expected to increase, a warmer climate forces more precipitation to fall as rain than snow resulting in a decrease in snowpack where larger and more frequent rainfall events occurring on shallower snowpacks during winter (Diffenbaugh et al., 2013). In the Pacific Northwest, for example, snowpack is predicted to decrease by 70% by 2100 under the RCP 8.5 scenario, even though annual precipitation may increase by 10% (Ikeda et al., 2021). Previous studies predicted declines in snowmelt-related flooding in the western United States and Canada, due to projected reductions in spring snowpack with warmer temperatures (Hamlet & Lettenmaier, 2007; Loukas et al., 2002). However, ROS and mixed-phase precipitation on snow events are becoming more frequent (McCabe et al., 2007) and are expected to continue in the future, particularly in regions with higher elevations (Li et al., 2019; Musselman et al., 2018; Yan et al., 2019). Davenport et al. (2020) also found that winter precipitation shifts toward rain, in response to warming, causing nonlinear increases in flood size across the western United States indicating that ROS events driven by larger and more frequent rainfall can result in increasing winter or spring floods.

Future projections of snow-related variables have been investigated using different modeling techniques across multiple time and space scales, including global climate models (GCMs; Brown & Mote, 2009; Krasting et al., 2013; Mudryk et al., 2020), regional climate models (RCMs; Mahoney et al., 2021; McCrary & Mearns, 2019; Rasmussen et al., 2011), and statistical downscaling applied to hydrologic land surface models (Christensen & Lettenmaier, 2007). Due to computational constraints, trade-offs must be made in most climate modeling approaches between the size of the simulation domain, model resolution, the number of climate models (RCMs or GCMs). The North American Coordinated Regional Climate Downscaling Experiment (NA-CORDEX; Mearns et al., 2017) ensemble of RCMs provides a unique opportunity to examine future changes over a large domain (all of North America) at relatively high resolutions (25 km) compared to GCMs, for historical and future time horizons from 1950 to 2100. Additionally, the relatively large number of RCM simulations in NA-CORDEX allows for the exploration of uncertainty (e.g., Kim et al., 2021), highlighting locations where additional studies may be needed to better understand the impacts of future change over North America.

Although many previous studies have been conducted to predict future changes in SWE and snowmelt in the United States and Canada, projected changes in extreme SWE, snowmelt, and RP across North America remains poorly understood. In this study, we create and compare spatial maps of three extreme design

metrics, SWE, snowmelt, RP (snowmelt plus precipitation), for the historical, mid, and late 21st centuries, respectively, using NA-CORDEX. The RP is the actual amount of water available for runoff originating from melting snow and precipitation (including snowfall, rainfall absorbed by the snowpack, and percolated rain water through the snowpack) for a given time period (Cho & Jacobs, 2020; Yan et al., 2018, 2019). We aim to answer the following three research questions: (a) How much will the magnitude of extreme SWE, snow melt, and RP change by the mid and late 21st century? (b) Are there similar spatial patterns among the three extreme design metrics across North America? (c) Which regions have the largest differences (uncertainty) among RCM models in future conditions?

2. Data and Methodology

2.1. Regional Climate Modeling (RCM) Framework

NA-CORDEX aims to add value to our understanding of climate change at regional scales to serve the climate change impact and adaptation communities (Mearns et al., 2017). In this study, daily 25-km spatial resolution SWE and precipitation from nine NA-CORDEX simulations, which follow the RCP 8.5 scenario, are used to examine changes in extreme SWE, snowmelt, and RP. The nine simulations from three RCMs with seven GCMs are summarized in Table S1 and Text S1 in Supporting Information S1. To offer additional information about the reliability of the NA-CORDEX, the 25-year return level NA-CORDEX SWE map is compared to the reference map over the continental United States, which was adopted from Cho and Jacobs (2020) (Figure S1 in Supporting Information S1).

2.2. Annual Maximum SWE, Snowmelt, and Runoff Potential

The term "extreme" values (or events) used in this study comes from extreme value theory that is widely used to estimate the probability of an unusually large event and the magnitude of the large event for a certain probability (Castillo, 2012). The 25-year return period design SWE and 7-day snowmelt and RP values are computed using the Generalized Extreme Value (GEV) frequency analysis approach with the annual maximum series of each variable (Hosking et al., 1990). The GEV distribution function with detailed explanations can be found in Text S2 in Supporting Information S1. The gridded, daily time series for each NA-CORDEX simulation ensemble was used to obtain the annual maximum SWE, snowmelt, and RP values and to calculate the corresponding design extreme values for historical (1976–2005), mid (2040–2069), and late (2070–2099) periods. Annual maximum SWE values are the one-day maximum value determined for each grid cell daily SWE time series from the October 1 to May 31. Annual maximum 7-day snowmelt and RP values are also obtained in that period. A 7-day duration is used to calculate the extreme design (25-year return level) snowmelt and RP based on general time periods of a response of streamflow to precipitation across the U.S. watersheds (Davenport et al., 2020; Ivancic & Shaw, 2015) and persistence days (i.e., multiple days to more than a week) of the historical snowmelt and ROS flood events (Pomeroy et al., 2016; Todhunter et al., 2001). The annual maximum 7-day RP is calculated by including precipitation into the amount of snow ablation (e.g., ROS). RP is defined as the actual amount of water available for runoff from the melting snow and precipitation (Yan et al., 2018).

Annual maximum 7-day snowmelt ($\text{Melt}_{\text{max}, 7\text{d}}$) for each grid is defined as

$$\text{Melt}_{\text{max},7} = \max\left[\text{SWE}_i - \text{SWE}_{i+7}\right] \text{ when } \text{SWE}_i - \text{SWE}_{i+7} > 0 \qquad (1)$$

Annual maximum 7-day RP ($\text{RP}_{\text{max}, 7\text{d}}$) includes precipitation, defined as

$$\text{RP}_{\text{max},7} = \max\left[\text{Prec}_{i+1\,\text{to}\,i+7} - \left(\text{SWE}_i - \text{SWE}_{i+7}\right)\right] \text{ when } \text{SWE}_i - \text{SWE}_{i+7} > 0 \qquad (2)$$

where i is a date from October 01 to May 31 for each year and SWE_i and SWE_{i+7} is daily SWE (mm) at dates, i and $i + 7$, respectively. $\text{Prec}_{i+1\,\text{to}\,i+7}$ is accumulated precipitation (mm) between i and $i + 7$ dates. To only consider snow-related events, the annual maximum values ($\text{Melt}_{\text{max},7}$ or $\text{RP}_{\text{max},7}$) are selected when positive $\text{SWE}_i - \text{SWE}_{i+7}$ (e.g., snow ablation) exists only. As compared to changes in SWE itself, the RP is a more relevant variable for quantifying the amount of water available to contribute to runoff processes and floods.
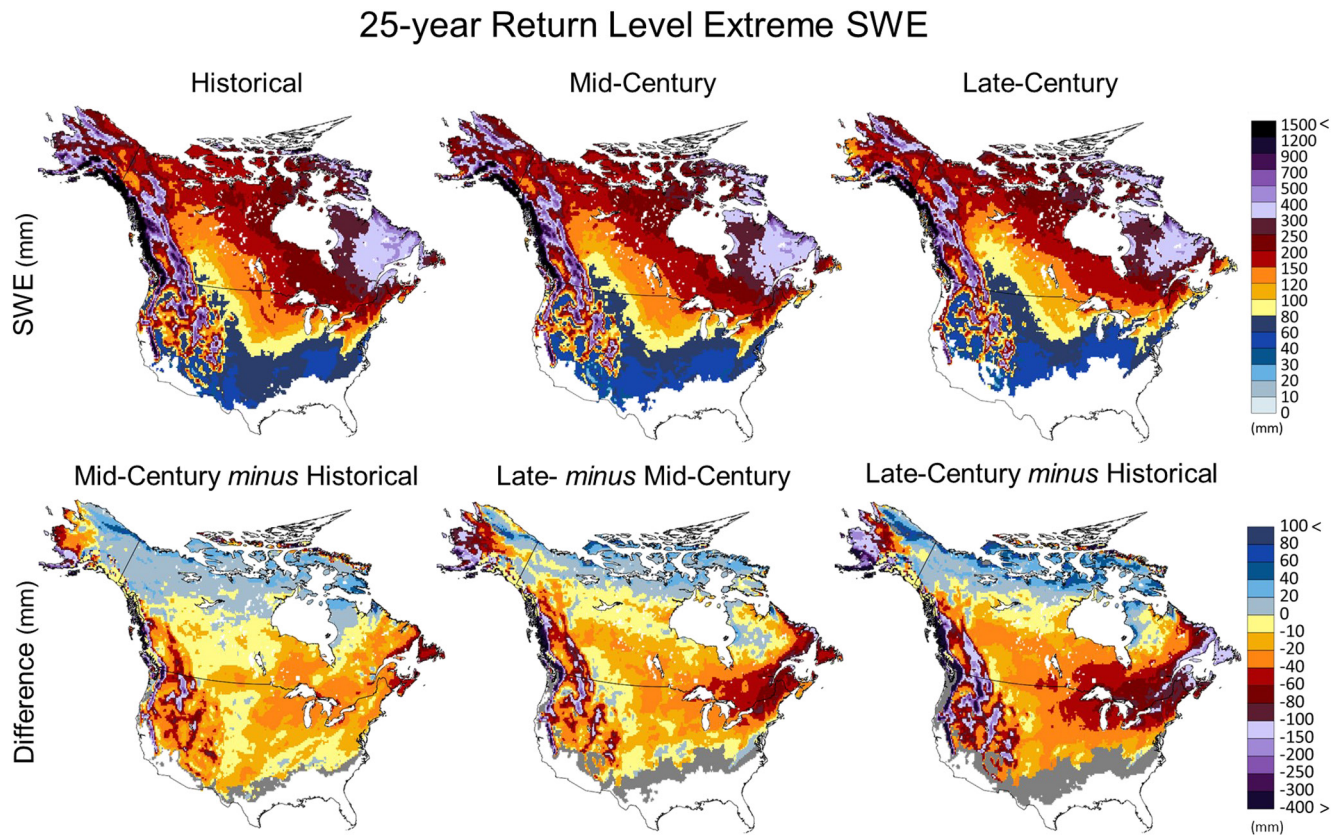
25-year Return Level Extreme SWE

Figure 1. Twenty-five-year return level design snow water equivalent (SWE) using the annual maximum SWE values for the historical (1976–2005), mid (2040–2069), and late (2070–2099) century and their difference maps. Gray color along the southern edge in the difference maps indicates regions where the SWE no longer exists.

In previous studies, this concept was often referred to using terms such as "water available for runoff" (Yan et al., 2019) and "surface water input" (Kormos et al., 2014). The RP calculation used in this study is based on the mass balance of snowpack (adopted in Yan et al., 2018), Runoff Potential (output) = Precipitation (input) − ΔSWE (storage change), indicating that the RP includes water available for runoff from the ROS events as well as the mixed-phase precipitation events on snow. While magnitude is the major focus of the study, the timing of annual maximum SWE, snowmelt, and RP are also a crucial part of the impact from snow changes. The average date of annual maximum SWE, snowmelt, and RP averaged over the historical and future periods, as well as their future changes are provided in Figure S2 in Supporting Information S1.

3. Results and Discussion

3.1. Projected Changes in Extreme SWE

The 25-year return level design SWE maps for the historical (1976–2005), mid (2040–2069), and late (2070–2099) century are presented with the difference maps among the three periods (Figure 1). In the historical period, large extreme SWE values exist in the Cascades in the Pacific Northwest, Rocky Mountains, eastern Taiga in Canada (dark purple and black). Low SWE values are distributed over the southern United States and Great Plains (blue colors). These spatial patterns are retained in future periods, but the magnitude of extreme SWE is projected to change. Large reductions in extreme SWE (up to 150 and 400 mm for the mid and late 21st century, respectively) are projected to occur over the western United States and Canada, southwest Alaska, and coastal eastern Canada (with the greatest changes in the Pacific Northwest and the Rocky Mountains). Extreme SWE is also projected to decrease in the Great Plains, the northeastern United States, Quebec, and Newfoundland and Labrador. The decrease in extreme SWE is consistent with previous studies that there are projected reductions in mean SWE or April 01 SWE across the regions (Demaria et al., 2016;

Li et al., 2017). Contrary to these regions, SWE extremes are projected to increase across high-latitude areas of Canada and northern Alaska. The patterns generally correspond to the net winter snowfall projection in Mankin and Diffenbaugh (2015). This is likely because warmer temperatures in extremely cold regions will increase snowfall by increasing winter precipitation and available moisture (Brown et al., 2017; Cohen et al., 2012; Mankin & Diffenbaugh, 2015). An increase in available moisture results in higher precipitation efficiency over northern Canada, where the air temperature is still sufficiently cold enough to yield snowfall (Ghatak et al., 2010). In most regions, the changes in SWE are more notable in the latter part of the century.

The magnitude of SWE decline is accompanied by a shift in the timing of peak SWE that occurs on average, 12 days earlier than the historical period by midcentury (2040–2069) and 20 days earlier than the historical period by the late century (2070–2099) across North America. In the Rocky Mountains, the Pacific Northwest, and the southwest Alaska, the timing of the peak SWE is projected to shift earlier by up to 48, 57, and 80 days by the end of the century, respectively.

3.2. Projected Changes in Extreme Snowmelt and Runoff Potential

The 25-year return level 7-day snowmelt maps have similar spatial patterns to those of the extreme SWE maps where regions with high SWE have large snowmelt (Figure 2a). Large snowmelt occurs in the Cascades, Rocky Mountains, eastern Taiga in Canada. Projected changes in the extreme snowmelt between the historical and future periods indicate that decreases will extend over the continental United States, southern Canada, and Alaska. The greatest changes are found in the western mountainous regions. In the North Cascades, e.g., the magnitude of extreme 7-day snowmelt is expected to decline by 100 mm/7-day and occur more than 70 days earlier in the season by the end of the century (Figure S2 in Supporting Information S1). Similar to the spatial pattern in extreme SWE, extreme snowmelt is also projected to increase across high-latitude areas of Canada and Northern Alaska (Brown et al., 2017). The resultant increase of snowmelt in these regions is nearly equal to the SWE increase. The degree of the projected changes in snowmelt from historical to midcentury and mid to late century also varies by region. In the northern Canada, much of the increasing snowmelt will occur by midcentury (35%) with modest changes for the remainder of the century (18% of regional mean values), while the eastern region's decrease in the melt is greater in the latter portion of the study period (19% relative to 10% in the earlier portion). In the western United States, the changes appear to be continuous through the late century (Midcentury *minus* Historical versus Late century *minus* Midcentury).

Despite the projected reduction in extreme SWE and snowmelt, future changes in extreme RP show that including ROS generally moderates the changes in SWE meltwater extremes in many regions or even increases RP (Figure 2b). Over the Sierra Nevada, Cascade Range, and the southeast United States, large increases in RP are projected by the end of the century. In the Sierra Nevada region, there is a notable increase in extreme RP by 22% (32%) but the timing of annual maximum RP occurs on average 23 (35) days earlier by the mid (late) century. In the Cascade Mountain range, the changes in extreme RP are mixed in midcentury (e.g., increases in southern British Columbia, but decreases in Oregon), but at the end of the century, there are consistent increases across the entire region. More than a 50 mm/7-day increase in the extreme RP is projected over northern Canada with RP extremes occurring later in the year.

The spatial distributions in the extreme RP, calculated by the annual maximum values of 7-day snowmelt combined with precipitation (e.g., ROS events), are different from those of the extreme snowmelt (Figure 2c). The RP values exceed the snowmelt values by up to 400 mm/7-day in the Pacific Northwest, California, and the southeast United States. This indicates that large precipitation events on snowpacks are the major contributor to extreme RP in these regions. In the northern Rocky Mountains and southern Alaska, the differences between RP and snowmelt gradually increase from the historical to mid and late centuries, indicating that the magnitude of liquid precipitation during the snow melt period will increasing. This is attributed in part to increasing temperatures that will lead to a shift in precipitation partitioning from snow to rain, particularly for western maritime regions. This has important implications for future spring and midwinter floods, which will likely increase in magnitude due to the reduced snow-precipitation ratios across western North America (Davenport et al., 2020). Flooding from only snowmelt will decrease in the future, but flooding induced by rain or mixed-phase precipitation in tandem with melting snowpack will increase in midwinter and spring. Increases in total winter and spring precipitation in some regions could
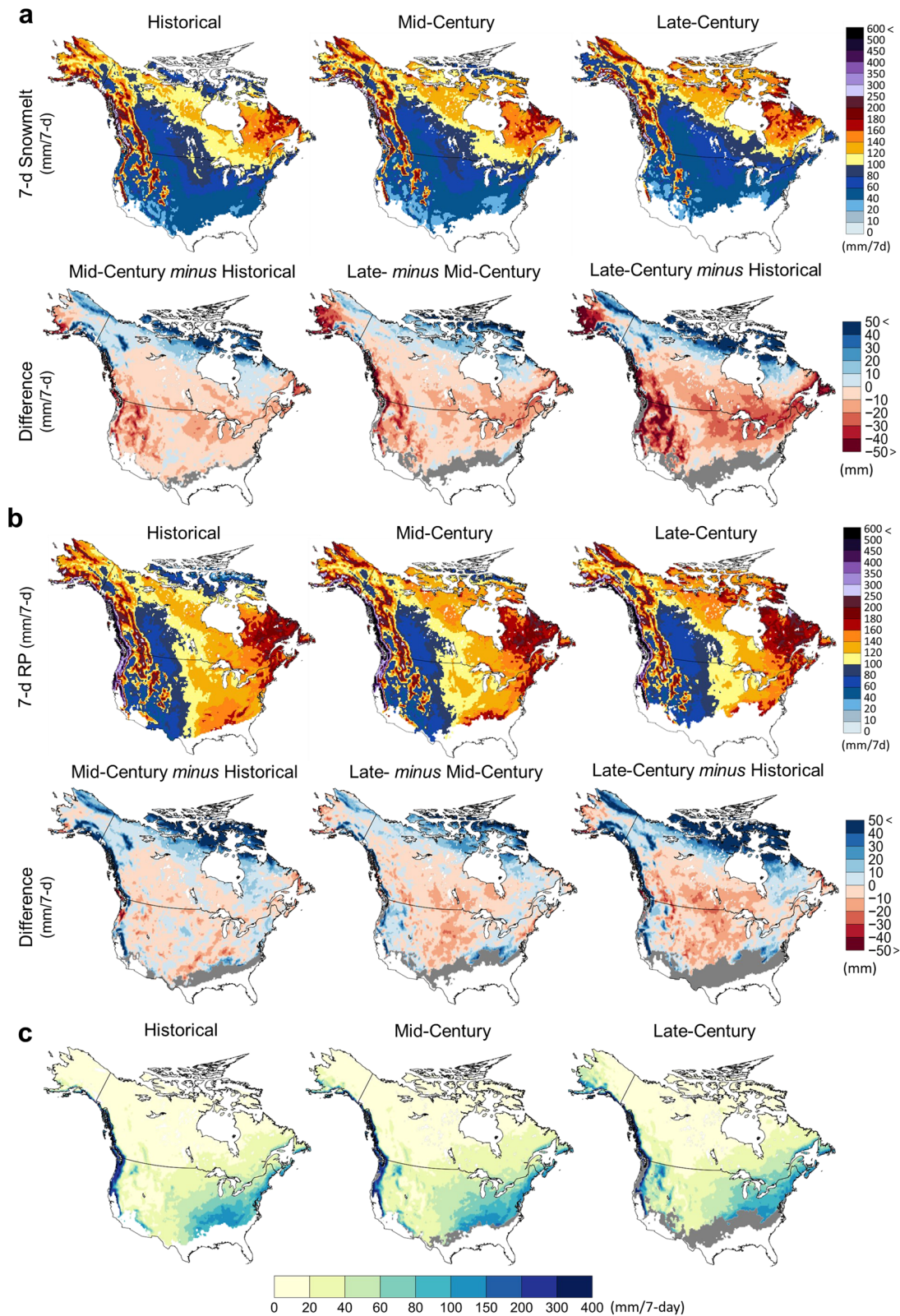
Figure 2. Twenty-five-year return level (a) 7-day snowmelt and (b) Runoff potential (RP) maps with difference maps for the historical (1976–2005), mid (2040–2069), and late (2070–2099) century and (c) Difference maps between 7-day RP and snowmelt for each period (gray color along the southern edge in the difference maps indicates regions where snowmelt (or RP) used to exist, but no longer exists).

additionally contribute to increases in the magnitude of future spring or midwinter floods (Bukovsky & Mearns, 2020; Mahoney et al., 2021). For example, in the Pacific Northwest and California, increases in total precipitation are projected in mountain valleys and on the lee-side of the mountains due to an increase in intense atmospheric river-driven precipitation (Huang et al., 2020). Also, early-season flood risk is expected to increase in association with increased runoff over heavy-rainy days in California's Sierra Nevada (Huang et al., 2018). In the midelevations (1,500–2,500 m), the runoff intensity is projected to increase by 50% and the frequency rises four times relative to the historical values under the RCP 8.5.

Even though changes in streamflow are not directly investigated in this study, we can extrapolate from recent studies that some areas can experience increases in streamflow even with earlier snowmelt and snowloss (Hammond & Kampf, 2020; McCabe et al., 2018; Robles et al., 2021). For example, Hammond and Kampf (2020) found that in regions where subsurface water storage is high and evapotranspiration is low, increases in rainfall and mixed-phase precipitation during wet winter periods generates higher runoff efficiency (calculated by quickflow, also known as "direct runoff," divided by precipitation input) which compensates for the reduced streamflow that occurs with declining snowpacks. Regarding watersheds where more frequent winter snowmelt and ROS events are projected to occur and where winter conditions become wetter in the future, larger extreme RP may directly lead to higher runoff efficiency and larger quickflow, potentially increasing midwinter flood risk.

3.3. Variations of SWE, Snowmelt, and RP Among RCMs

To identify regions where there is the largest variability among RCMs, the variability in the ensemble spread (standard deviation among nine ensemble members) of extreme SWE, snowmelt, and RP across North America is examined in Figure 3. Coefficient of variation (CV) maps are also provided in Figure S2 in Supporting Information S1, which is calculated by dividing the standard deviation by the ensemble mean. For SWE, the largest uncertainty is in the western mountain regions including the Pacific Northwest and the Rocky Mountains. This is primarily due to the larger magnitude of SWE and differences among RCMs to characterize SWE for regions with complex terrain characteristics. As demonstrated in Figure S1 in Supporting Information S1, the RCMs generally underestimate extreme SWE values as compared to an SWE reference data set in these regions. This is likely because the 25-km spatial resolution of the RCMs, while much finer than GCM scales, is still too coarse to represent local heterogeneous processes for snow, especially in complex terrains (Ikeda et al., 2021; Letcher & Minder, 2015; Wrzesien et al., 2017, 2018). RCM SWE output at a finer resolution (<9 km) compares favorably to reference SWE data sets as compared to the output at 27 km (Wrzesian et al., 2017). Even higher resolution RCM experiments (~4 km) enable to model microphysical features such as orographical updrafts driving clouds and precipitation (e.g., Ikeda et al., 2021; Rasmussen et al., 2014). For the CV maps of SWE, there is a relatively large variation in the central and southern parts of the United States (Figure S2 in Supporting Information S1). While the large uncertainty in these regions would be less important in terms of extreme events, it can limit the predictability of agricultural and ecological processes related to snowmelt (Petersky & Harpold, 2018).

For snowmelt, there are large variabilities in both the western mountain regions and northern Canada. With limited SWE variations in northern Canada, the larger variability in snowmelt is likely due to the temperature differences among the RCMs. Because a large increase in precipitation (up to 46%) in northern Canada is expected in the late 21st century (Zhang et al., 2019), this region could be more vulnerable to snow-driven floods than other regions. The RP maps show larger uncertainties in the southern parts of the United States, which are up to 70 mm/7 day for historical and midcentury. In the late 21st century, SWE no longer exists in the regions. Because ephemeral snowpack changes in these regions are important for hydrologic and ecosystem processes (Cho & Jacobs, 2020; Friggens et al., 2018), further study to better understand the source of these uncertainties is warranted. There are also large RP variations among RCMs in the Pacific Northwest and California where large shifts in precipitation partitioning from snowfall to rain as well as increases in extreme atmospheric river-induced precipitation are expected (Huang et al., 2020). Further investigation is needed to better understand and harness the RP ensemble spread and in those regions.

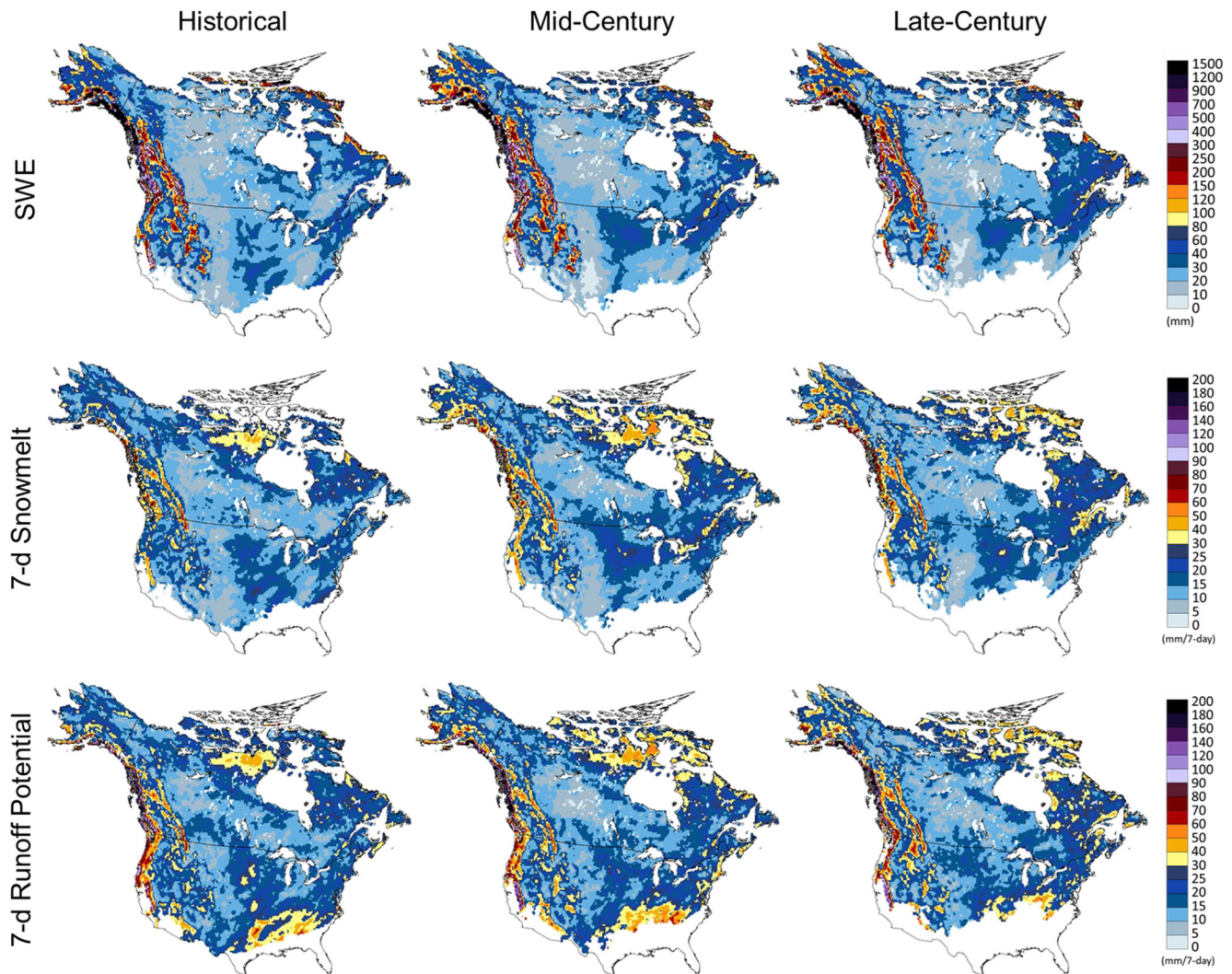## Standard deviation of the 25-year 9 RCM models

Figure 3. Standard deviations of the 25-year return level snow water equivalent (SWE), 7-day snowmelt, and runoff potential (RP) maps using the nine simulation outputs in the NA-CORDEX ensemble.

3.4. Regional Change in Extreme Snow-Driven Events

For design purposes, the granularity of the previous maps is not well suited for decision-makers seeking to change policies and engineering practice. Thus, the projected regional changes in the extreme SWE and 7-day snowmelt and RP results are summarized in Figure 4. Here, total volume change maps are provided for 14 regions based on the U.S. National Climate Assessment and Canada's Changing Climate Report boundaries. Projections show regional differences in changes to design SWE, snowmelt, and RP. Large decreases in extreme SWE are projected to occur over much of North America, except for Alaska and northern Canada (e.g., Yukon, Northwest Territories, and Nunavut). In the continental United States, projected extreme SWE decreases by 12–37% and 25–72% by mid and late 21st century, respectively. There is a relatively small decrease in southern Canada, ranging from 3% to 13% (midcentury) and 11% to 30% (late century). The widespread SWE decreases across the continental United States and southern Canada are mainly attributable to increasing temperatures that will shift the proportion of total precipitation that currently falls as snowfall toward rain (Sospedra-Alfonso & Merryfield, 2017). Projected increases in the extreme SWE in Alaska and northern Canada are due to larger increases in winter snowfall despite winter temperatures
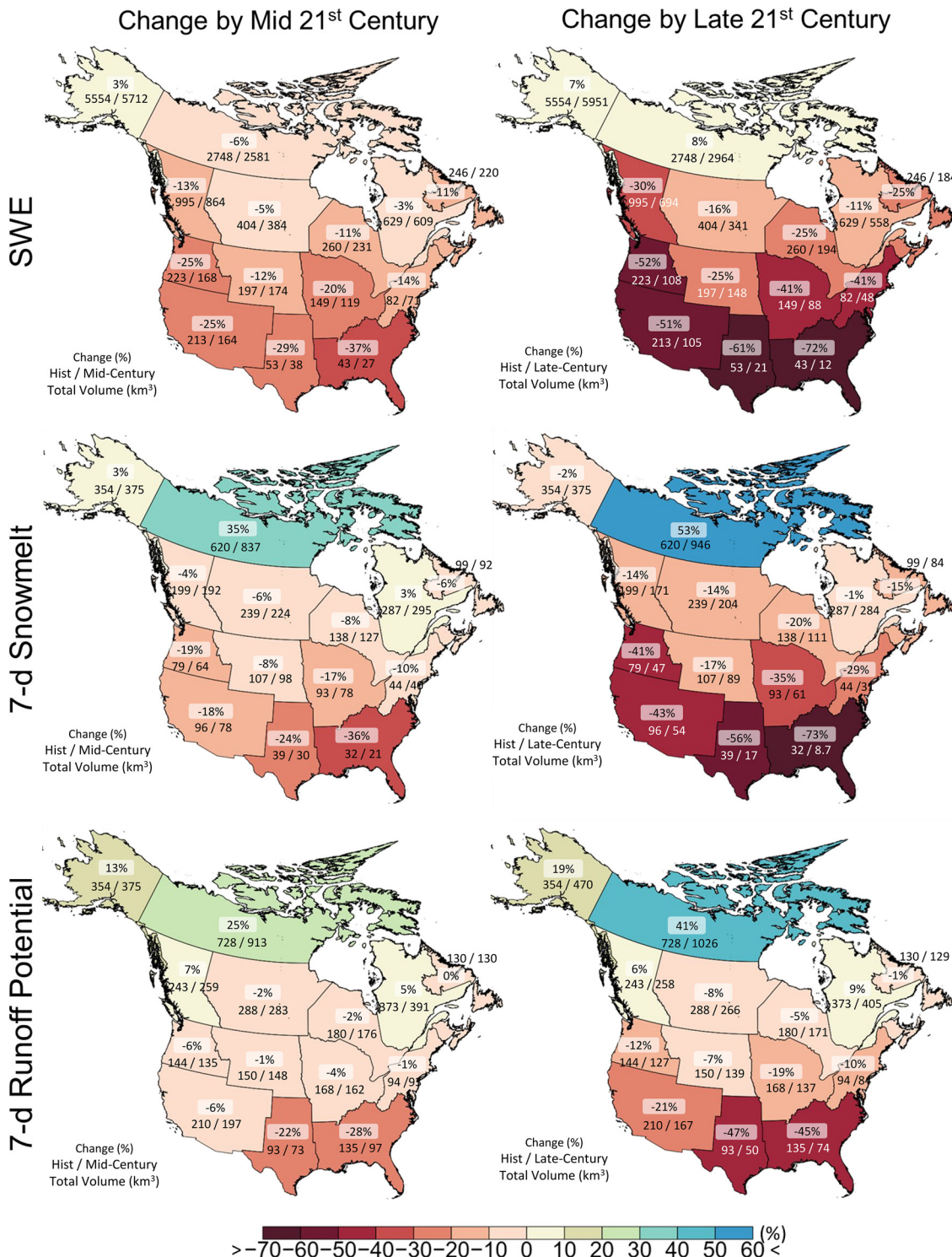
Figure 4. Projected changes in extreme snow water equivalent (SWE), 7-day snowmelt, and runoff potential (RP) over North America using the U.S. National Climate Assessment and Canada's Changing Climate Report boundaries.

warming by up to 4°C (Mankin & Diffenbaugh, 2015) because the winter temperature would be still sufficiently cold to generate snowfall (Ghatak et al., 2010).

Regional changes in the future extreme snowmelt generally have similar spatial patterns to those of the maximum SWE. However, there is a notable difference in projected snowmelt between northern and southern Canada. Even though there are minimal increases in extreme SWE in the high-latitude areas of Canada (Brown et al., 2017; Mudryk et al., 2018), extreme snowmelt is projected to increase significantly by 35% and 53% by the mid and late 21st century, respectively. Here, warmer temperatures and reduced snowpacks combine to affect the magnitude of snowmelt-related events, which was noted as an uncertain issue in the recent Canada's Changing Climate Report (Bush & Lemmen, 2019). In the continental United States and southern Canada, the smaller SWE, rather than warmer temperature, is the more important control that causes smaller snowmelt events, while in northern Canada the warmer temperatures drive the larger increases in snowmelt for regions with similar or slightly larger SWE.

For extreme RP, there are increases in northern Canada (25% and 41%) as well as Alaska (13% and 19% by mid and late centuries, respectively). Projected RP changes are consistent but smaller than projected snowmelt reductions in the continental United States. Contrary to the decrease in snowmelt, there is a projected increase in extreme RP in British Columbia (7% and 6% by mid and late centuries, respectively) even though extreme SWE decreases. Similar increases also occur in the Pacific Coast Ranges of western North America (in Figure 2). Considering that winter precipitation in the regions is projected to increase by up to 20% from the U.S. National Climate Assessment (Easterling et al., 2017), the RP increase is likely caused by two reasons: an increase in winter precipitation itself and a large portion of snowfall being replaced by rain in response to climate warming (Mankin & Diffenbaugh, 2015). The relative contributions of the drivers may differ by region with elevation ranges because of the elevation-dependent warming and resultant precipitation phases (Ding et al., 2014; Pepin et al., 2015).

4. Conclusion and Future Perspectives

While it is well known that a warmer climate will cause widespread decreases in snowpack and snowmelt across North America, previous studies have not translated these projected changes to extreme values appropriate for water resources management and engineering design. In this study, 25-year return level design SWE and 7-day snowmelt and RP were estimated for the historic, mid, and late 21st century using a nine-member RCM ensemble from NA-CORDEX. We found that the magnitude of extreme SWE decreases range from 3%–37% to 11%–72% across the continental United States and southern Canada by mid and late 21st century, respectively, except for a small increase of about 8% in Alaska and northern Canada. Generally, the magnitude of extreme snowmelt is informed by the amount of SWE that is present before melting events occur. However, in the high-latitude areas of Canada extreme snowmelt is projected to markedly increase by 35% and 53% by the mid and late century, even though there will be marginal increases in extreme SWE. In California and the Pacific Northwest regions, there is a notable increase in extreme RP by 21% contrary to a decrease in snowmelt itself by −31% by the end of the 21st century. This is probably attributable to an increasing temperature that will lead to a shift in the proportion of precipitation partitioning toward rainfall, suggesting that these regions may be vulnerable to ROS events in a changing climate. Based on the ensemble spread among the nine RCM models, we found the western mountain regions have the greatest uncertainties among the models for extreme SWE. For snowmelt, large variabilities were found in both the western mountain regions and northern Canada. With small SWE variations in northern Canada, the variability in snowmelt is likely due to the temperature differences among the RCMs. For extreme RP, there are also large uncertainties in the southeastern United States, requiring further investigation to identify potential sources of these regional differences in the RCM's ephemeral snow estimates.

One limitation for this study is the use of a relatively course spatial resolution (25 km) climate simulations, for the study of changes in snow in complex terrain. The need of reliable, high resolution climate modeling to capture local climate processes for snow in complex terrains (e.g., mountains) has been mentioned before. Considering the inevitable trade-offs among the size of the simulation domain, model resolution, and the number of climate models, mostly due to limited computational resources, the 25-km spatial resolution of the NA-CORDEX ensemble simulations is still enough to project regional snowpack changes with an

ensemble that is large enough to explore some uncertainty across North America. The large coverage of the NA-CORDEX simulations allows us to compare how changes vary across the domain and to identify where additional studies may be needed to better understand the impacts of future change. The results from this study are expected to provide useful information regarding the magnitude of future snow-driven extremes under a changing climate as needed to plan, design, and manage potentially vulnerable water resources management and infrastructure standards.

Data Availability Statement

The NA-CORDEX data used in this study are publicly available at the Climate Data Gateway at National Center for Atmospheric Research (https://www.earthsystemgrid.org/search/cordexsearch.html). The 25-year return level SWE, snowmelt, and RP maps and their standard deviation and coefficient of variation maps developed in this study are available in Hydroshare and can be accessed at https://www.hydroshare.org/resource/8efb0f7e743f4a11a4da8b045a37165b

References

Barnett, T. P., Adam, J. C., & Lettenmaier, D. P. (2005). Potential impacts of a warming climate on water availability in snow-dominated regions. *Nature*, *438*(7066), 303–309. https://doi.org/10.1038/nature04141

Berghuijs, W. R., Woods, R. A., Hutton, C. J., & Sivapalan, M. (2016). Dominant flood generating mechanisms across the United States. *Geophysical Research Letters*, *43*, 4382–4390. https://doi.org/10.1002/2016GL068070

Brown, R., Schuler, D., Bulygina, O., Derksen, C., Luojus, K., Mudryk, L., et al. (2017). Arctic terrestrial snow. In *Snow water ice and permafrost in the Arctic (SWIPA) 2017 assessment* (p. 40). Arctic Monitoring and Assessment Programme.

Brown, R. D., & Mote, P. W. (2009). The response of Northern Hemisphere snow cover to a changing climate. *Journal of Climate*, *22*(8), 2124–2145. https://doi.org/10.1175/2008jcli2665.1

Bukovsky, M. S., & Mearns, L. O. (2020). Regional climate change projections from NA-CORDEX and their relation to climate sensitivity. *Climatic Change*, *162*(2), 645–665. https://doi.org/10.1007/s10584-020-02835-x

Bush, E., & Lemmen, D. S. (2019). *Canada's changing climate report*. Government of Canada=Gouvernement du Canada.

Castillo, E. (2012). *Extreme value theory in engineering*. Elsevier.

Cho, E., & Jacobs, J. M. (2020). Extreme value snow water equivalent and snowmelt for infrastructure design over the contiguous United States. *Water Resources Research*, *56*, e2020WR028126. https://doi.org/10.1029/2020WR028126

Christensen, N. S., & Lettenmaier, D. P. (2007). A multimodel ensemble approach to assessment of climate change impacts on the hydrology and water resources of the Colorado River Basin. *Hydrology and Earth System Sciences*, *11*(4), 1417–1434. https://doi.org/10.5194/hess-11-1417-2007

Cohen, J. L., Furtado, J. C., Barlow, M. A., Alexeev, V. A., & Cherry, J. E. (2012). Arctic warming, increasing snow cover and widespread boreal winter cooling. *Environmental Research Letters*, *7*(1), 014007. https://doi.org/10.1088/1748-9326/7/1/014007

Davenport, F. V., Herrera-Estrada, J. E., Burke, M., & Diffenbaugh, N. S. (2020). Flood size increases nonlinearly across the Western United States in response to lower snow-precipitation ratios. *Water Resources Research*, *56*, e2019WR025571. https://doi.org/10.1029/2019WR025571

Demaria, E. M., Roundy, J. K., Wi, S., & Palmer, R. N. (2016). The effects of climate change on seasonal snowpack and the hydrology of the northeastern and upper Midwest United States. *Journal of Climate*, *29*(18), 6527–6541. https://doi.org/10.1175/jcli-d-15-0632.1

Diffenbaugh, N. S. (2017). *What California's dam crisis says about the changing climate*. The New York Times. Retrieved from https://www.nytimes.com/2017/02/14/opinion/what-californias-dam-crisis-says-about-the-changing-climate.html

Diffenbaugh, N. S., Scherer, M., & Ashfaq, M. (2013). Response of snow-dependent hydrologic extremes to continued global warming. *Nature Climate Change*, *3*(4), 379–384. https://doi.org/10.1038/nclimate1732

Ding, B., Yang, K., Qin, J., Wang, L., Chen, Y., & He, X. (2014). The dependence of precipitation types on surface elevation and meteorological conditions and its parameterization. *Journal of Hydrology*, *513*, 154–163. https://doi.org/10.1016/j.jhydrol.2014.03.038

Easterling, D. R., Kunkel, K. E., Arnold, J. R., Knutson, T., LeGrande, A. N., Leung, L. R., et al. (2017). Precipitation change in the United States. In D. J. Wuebbles, D. W. Fahey, K. A. Hibbard, D. J. Dokken, B. C. Stewart, & T. K. Maycock (Eds.), *Climate science special report: Fourth national climate assessment* (Vol. *I*, pp. 207–230). U.S. Global Change Research Program. https://doi.org/10.7930/J0H993CC

Fassnacht, S. R., & Records, R. M. (2015). Large snowmelt versus rainfall events in the mountains. *Journal of Geophysical Research: Atmospheres*, *120*, 2375–2381. https://doi.org/10.1002/2014JD022753

Friggens, M. M., Williams, M. I., Bagne, K. E., Wixom, T. T., & Cushman, S. A. (2018). Effects of climate change on terrestrial animals. In Halofsky, J. E., Peterson, D. L., Ho, J. J., Little, N., Joyce, L. A., et al. (Eds.), *Climate change vulnerability and adaptation in the Intermountain Region [Part 2]. Gen. Tech. Rep. RMRS-GTR-375* (Chap. 9, Vol. *375*, pp. 264–315). US Department of Agriculture, Forest Service, Rocky Mountain Research Station.

Ghatak, D., Frei, A., Gong, G., Stroeve, J., & Robinson, D. (2010). On the emergence of an Arctic amplification signal in terrestrial Arctic snow extent. *Journal of Geophysical Research*, *115*, D24105. https://doi.org/10.1029/2010JD014007

Hamlet, A. F., & Lettenmaier, D. P. (2007). Effects of 20th century warming and climate variability on flood risk in the western US. *Water Resources Research*, *43*, W06427. https://doi.org/10.1029/2006WR005099

Hammond, J. C., & Kampf, S. K. (2020). Subannual streamflow responses to rainfall and snowmelt inputs in snow-dominated watersheds of the western United States. *Water Resources Research*, *56*, e2019WR026132. https://doi.org/10.1029/2019WR026132

Harpold, A. A., & Kohler, M. (2017). Potential for changing extreme snowmelt and rainfall events in the mountains of the western United States. *Journal of Geophysical Research: Atmospheres*, *122*, 13219–13228. https://doi.org/10.1002/2017JD027704

Henn, B., Musselman, K. N., Lestak, L., Ralph, F. M., & Molotch, N. P. (2020). Extreme runoff generation from atmospheric river driven snowmelt during the 2017 Oroville Dam spillways incident. *Geophysical Research Letters*, *47*, e2020GL088189. https://doi.org/10.1029/2020GL088189

Hosking, J. R. M. (1990). L-moments: Analysis and estimation of distributions using linear combinations of order statistics. *Journal of the Royal Statistical Society: Series B*, *52*(1), 105–124. https://doi.org/10.1111/j.2517-6161.1990.tb01775.x

Huang, X., Hall, A. D., & Berg, N. (2018). Anthropogenic warming impacts on today's Sierra Nevada snowpack and flood risk. *Geophysical Research Letters*, *45*, 6215–6222. https://doi.org/10.1029/2018GL077432

Huang, X., Swain, D. L., & Hall, A. D. (2020). Future precipitation increase from very high resolution ensemble downscaling of extreme atmospheric river storms in California. *Science Advances*, *6*(29), eaba1323. https://doi.org/10.1126/sciadv.aba1323

Ikeda, K., Rasmussen, R., Liu, C., Newman, A., Chen, F., Barlage, M., et al. (2021). Snowfall and snowpack in the Western US as captured by convection permitting climate simulations: Current climate and pseudo global warming future climate. *Climate Dynamics*, *57*, 2191–2215. https://doi.org/10.1007/s00382-021-05805-w

Ivancic, T. J., & Shaw, S. B. (2015). Examining why trends in very heavy precipitation should not be mistaken for trends in very high river discharge. *Climatic Change*, *133*(4), 681–693. https://doi.org/10.1007/s10584-015-1476-1

Kim, R. S., Kumar, S., Vuyovich, C., Houser, P., Lundquist, J., Mudryk, L., et al. (2021). Snow ensemble uncertainty project (SEUP): Quantification of snow water equivalent uncertainty across North America via ensemble land surface modeling. *The Cryosphere*, *15*(2), 771–791. https://doi.org/10.5194/tc-15-771-2021

Kormos, P. R., Marks, D., McNamara, J. P., Marshall, H. P., Winstral, A., & Flores, A. N. (2014). Snow distribution, melt and surface water inputs to the soil in the mountain rain-snow transition zone. *Journal of Hydrology*, *519*, 190–204. https://doi.org/10.1016/j.jhydrol.2014.06.051

Krasting, J. P., Broccoli, A. J., Dixon, K. W., & Lanzante, J. R. (2013). Future changes in Northern Hemisphere snowfall. *Journal of Climate*, *26*(20), 7813–7828. https://doi.org/10.1175/jcli-d-12-00832.1

Letcher, T. W., & Minder, J. R. (2015). Characterization of the simulated regional snow albedo feedback using a regional climate model over complex terrain. *Journal of Climate*, *28*(19), 7576–7595. https://doi.org/10.1175/jcli-d-15-0166.1

Li, D., Lettenmaier, D. P., Margulis, S. A., & Andreadis, K. (2019). The role of rain-on-snow in flooding over the conterminous United States. *Water Resources Research*, *55*, 8492–8513. https://doi.org/10.1029/2019WR024950

Li, D., Wrzesien, M. L., Durand, M., Adam, J., & Lettenmaier, D. P. (2017). How much runoff originates as snow in the western United States, and how will that change in the future? *Geophysical Research Letters*, *44*, 6163–6172. https://doi.org/10.1002/2017GL073551

Loukas, A., Vasiliades, L., & Dalezios, N. R. (2002). Potential climate change impacts on flood producing mechanisms in southern British Columbia, Canada using the CGCMA1 simulation results. *Journal of Hydrology*, *259*(1–4), 163–188. https://doi.org/10.1016/s0022-1694(01)00580-7

Mahoney, K., Scott, J. D., Alexander, M., McCrary, R., Hughes, M., Swales, D., & Bukovsky, M. (2021). Cool season precipitation projections for California and the Western United States in NA-CORDEX models. *Climate Dynamics*, *56*, 3081–3102. https://doi.org/10.1007/s00382-021-05632-z

Mankin, J. S., & Diffenbaugh, N. S. (2015). Influence of temperature and precipitation variability on near-term snow trends. *Climate Dynamics*, *45*(3), 1099–1116. https://doi.org/10.1007/s00382-014-2357-4

McCabe, G. J., Clark, M. P., & Hay, L. E. (2007). Rain-on-snow events in the western United States. *Bulletin of the American Meteorological Society*, *88*(3), 319–328. https://doi.org/10.1175/bams-88-3-319

McCabe, G. J., Wolock, D. M., & Valentin, M. (2018). Warming is driving decreases in snow fractions while runoff efficiency remains mostly unchanged in snow-covered areas of the western United States. *Journal of Hydrometeorology*, *19*(5), 803–814. https://doi.org/10.1175/jhm-d-17-0227.1

McCrary, R. R., & Mearns, L. O. (2019). Quantifying and diagnosing sources of uncertainty in midcentury changes in North American snowpack from NARCCAP. *Journal of Hydrometeorology*, *20*(11), 2229–2252. https://doi.org/10.1175/jhm-d-18-0248.1

Mearns, L. O., McGinnis, S., Korytina, D., Arritt, R., Biner, S., Bukovsky, M., et al. (2017). *The NA-CORDEX dataset, version 1.0*. NCAR Climate Data Gateway. https://doi.org/10.5065/D6SJ1JCH

Mudryk, L., Santolaria-Otín, M., Krinner, G., Ménégoz, M., Derksen, C., Brutel-Vuilmet, C., et al. (2020). Historical Northern Hemisphere snow cover trends and projected changes in the CMIP6 multi-model ensemble. *The Cryosphere*, *14*(7), 2495–2514. https://doi.org/10.5194/tc-14-2495-2020

Mudryk, L. R., Derksen, C., Howell, S., Laliberté, F., Thackeray, C., Sospedra-Alfonso, R., et al. (2018). Canadian snow and sea ice: Historical trends and projections. *The Cryosphere*, *12*(4), 1157–1176. https://doi.org/10.5194/tc-12-1157-2018

Musselman, K. N., Clark, M. P., Liu, C., Ikeda, K., & Rasmussen, R. (2017). Slower snowmelt in a warmer world. *Nature Climate Change*, *7*(3), 214–219. https://doi.org/10.1038/nclimate3225

Musselman, K. N., Lehner, F., Ikeda, K., Clark, M. P., Prein, A. F., Liu, C., et al. (2018). Projected increases and shifts in rain-on-snow flood risk over western North America. *Nature Climate Change*, *8*(9), 808–812. https://doi.org/10.1038/s41558-018-0236-4

Pepin, N., Bradley, R. S., Diaz, H. F., Baraër, M., Caceres, E. B., Forsythe, N., et al. (2015). Elevation-dependent warming in mountain regions of the world. *Nature Climate Change*, *5*(5), 424–430. https://doi.org/10.1038/nclimate2563

Petersky, R., & Harpold, A. (2018). Now you see it, now you don't: A case study of ephemeral snowpacks and soil moisture response in the Great Basin, USA. *Hydrology and Earth System Sciences*, *22*(9), 4891–4906. https://doi.org/10.5194/hess-22-4891-2018

Pomeroy, J. W., Stewart, R. E., & Whitfield, P. H. (2016). The 2013 flood event in the South Saskatchewan and Elk River basins: Causes, assessment and damages. *Canadian Water Resources Journal/Revue Canadienne Des Ressources Hydriques*, *41*(1–2), 105–117. https://doi.org/10.1080/07011784.2015.1089190

Rasmussen, R., Ikeda, K., Liu, C., Gochis, D., Clark, M., Dai, A., et al. (2014). Climate change impacts on the water balance of the Colorado headwaters: High-resolution regional climate model simulations. *Journal of Hydrometeorology*, *15*(3), 1091–1116. https://doi.org/10.1175/jhm-d-13-0118.1

Rasmussen, R., Liu, C., Ikeda, K., Gochis, D., Yates, D., Chen, F., et al. (2011). High-resolution coupled climate runoff simulations of seasonal snowfall over Colorado: A process study of current and warmer climate. *Journal of Climate*, *24*(12), 3015–3048. https://doi.org/10.1175/2010jcli3985.1

Robles, M. D., Hammond, J. C., Kampf, S. K., Biederman, J. A., & Demaria, E. (2021). Winter inputs buffer streamflow sensitivity to snowpack losses in the Salt River Watershed in the Lower Colorado River Basin. *Water*, *13*(1), 3. https://doi.org/10.3390/w13010003

Rokaya, P., Budhathoki, S., & Lindenschmidt, K. E. (2018). Trends in the timing and magnitude of ice-jam floods in Canada. *Scientific Reports*, *8*(1), 5834. https://doi.org/10.1038/s41598-018-24057-z

Sospedra-Alfonso, R., & Merryfield, W. J. (2017). Influences of temperature and precipitation on historical and future snowpack variability over the Northern Hemisphere in the Second Generation Canadian Earth System Model. *Journal of Climate*, *30*(12), 4633–4656. https://doi.org/10.1175/jcli-d-16-0612.1

Stadnyk, T., Dow, K., Wazney, L., & Blais, E.-L. (2016). The 2011 flood event in the Red River Basin: Causes, assessment and damages. *Canadian Water Resources Journal*, *41*(1–2), 65–64. https://doi.org/10.1080/07011784.2015.1009949

Todhunter, P. E. (2001). A hydroclimatological analysis of the Red River of the North snowmelt flood catastrophe of 1997. *JAWRA Journal of the American Water Resources Association*, *37*(5), 1263–1278. https://doi.org/10.1111/j.1752-1688.2001.tb03637.x

Vano, J. A., Miller, K., Dettinger, M. D., Cifelli, R., Curtis, D., Dufour, A., et al. (2019). Hydroclimatic extremes as challenges for the water management community: Lessons from Oroville dam and Hurricane Harvey. *Bulletin of the American Meteorological Society*, *100*(1), S9–S14. https://doi.org/10.1175/bams-d-18-0219.1

Villarini, G. (2016). On the seasonality of flooding across the continental United States. *Advances in Water Resources*, *87*, 80–91. https://doi.org/10.1016/j.advwatres.2015.11.009

Wrzesien, M. L., Durand, M. T., Pavelsky, T. M., Howat, I. M., Margulis, S. A., & Huning, L. S. (2017). Comparison of methods to estimate snow water equivalent at the mountain range scale: A case study of the California Sierra Nevada. *Journal of Hydrometeorology*, *18*(4), 1101–1119. https://doi.org/10.1175/jhm-d-16-0246.1

Wrzesien, M. L., Durand, M. T., Pavelsky, T. M., Kapnick, S. B., Zhang, Y., Guo, J., & Shum, C. K. (2018). A new estimate of North American mountain snow accumulation from regional climate model simulations. *Geophysical Research Letters*, *45*, 1423–1432. https://doi.org/10.1002/2017GL076664

Yan, H., Sun, N., Wigmosta, M., Leung, L. R., Hou, Z., Coleman, A., & Skaggs, R. (2019). Evaluating next-generation intensity-duration-frequency curves for design flood estimates in the snow-dominated western United States. *Hydrological Processes*, *34*, 1255–1268. https://doi.org/10.1002/hyp.13673

Yan, H., Sun, N., Wigmosta, M., Skaggs, R., Hou, Z., & Leung, R. (2018). Next-generation intensity-duration-frequency curves for hydrologic design in snow-dominated environments. *Water Resources Research*, *54*, 1093–1108. https://doi.org/10.1002/2017WR021290

Yarnal, B., Johnson, D. L., Frakes, B. J., Bowles, G. I., & Pascale, P. (1997). The flood of '96 and its socioeconomic impacts in the Susquehanna River Basin. *Journal of the American Water Resources Association*, *33*(6), 1299–1312. https://doi.org/10.1111/j.1752-1688.1997.tb03554.x

Zhang, X., Flato, G., Kirchmeier-Young, M., Vincent, L., Wan, H., Wang, X., et al. (2019). Changes in temperature and precipitation across Canada. In E.Bush, & D.S.Lemmen (Eds.), *Canada's changing climate report* (Chap. 4, pp. 112–193). Government of Canada.

References From the Supporting Information

Hernández-Díaz, L., Nikiéma, O., Laprise, R., Winger, K., & Dandoy, S. (2019). Effect of empirical correction of sea-surface temperature biases on the CRCM5-simulated climate and projected climate changes over North America. *Climate Dynamics*, *53*(1), 453–476. https://doi.org/10.1007/s00382-018-4596-2

McGinnis, S., & Mearns, L. (2021). Building a climate service for North America based on the NA-CORDEX data archive. *Climate Services*, *22*, 100233. https://doi.org/10.1016/j.cliser.2021.100233

Rhoades, A. M., Jones, A. D., & Ullrich, P. A. (2018a). Assessing mountains as natural reservoirs with a multimetric framework. *Earth's Future*, *6*, 1221–1241. https://doi.org/10.1002/2017EF000789

Rhoades, A. M., Jones, A. D., & Ullrich, P. A. (2018b). The changing character of the California Sierra Nevada as a natural reservoir. *Geophysical Research Letters*, *45*, 13008–13019. https://doi.org/10.1002/2017EF000789

Stedinger, J. R., Vogel, R. M., & Foufoula-Georgiou, E. (1993). Chapter 18 frequency analysis of extreme events. In D. R. Maidment (Ed.), *Handbook of hydrology* (pp. 1–66). DR McGraw-Hill. Retrieved from https://sites.tufts.edu/richardvogel/files/2019/04/frequencyAnalysis.pdf